

IS THE EQUATION OF STATE OF STRONGLY INTERACTING MATTER OBSERVABLE ?

OMAR BENHAR

INFN, Sezione di Roma

Dipartimento di Fisica, Università “La Sapienza”

I-00161 Roma, Italy

E-mail: benhar@roma1.infn.it

I review the available empirical information on the equation of state of cold strongly interacting matter, as well as the prospects for obtaining new insights from the experimental study of gravitational waves emitted by neutron stars.

1 Introduction

The equation of state (EOS) is a nontrivial relation linking the thermodynamic variables specifying the state of a physical system ¹. The best known example of EOS is Boyle’s *ideal gas law*, stating that the pressure of a collection of N noninteracting, pointlike classical particles, enclosed in a volume Ω , grows linearly with the temperature T and the average particle density $n = N/\Omega$.

The ideal gas law provides a good description of very dilute systems. In general, the EOS can be written as an expansion of the pressure, P , in powers of the density (we use units such that Boltzmann’s constant is $K_B = 1$):

$$P = nT [1 + nB(T) + n^2C(T) + \dots] . \quad (1)$$

The coefficients appearing in the above series, that goes under the name of *virial expansion*, are functions of temperature only. They describe the deviations from the ideal gas law and can be calculated in terms of the underlying elementary interaction. Therefore, the EOS carries a great deal of dynamical information, and its knowledge makes it possible to establish a link between measurable *macroscopic* quantities, such as pressure or temperature, and the forces acting between the constituents of the system at *microscopic* level.

This point is best illustrated by the van der Waals EOS, which describes a collection of particles interacting through a potential featuring a strong repulsive core followed by a weaker attractive tail (see fig.1). At $|U_0|/T \ll 1$, U_0 being the strength of the attractive part of the potential, the van der Waals EOS takes the simple form

$$P = \frac{nT}{1 - nb} - an^2 , \quad (2)$$

and the two quantities a and b , taking into account interaction effects, can be directly related to the potential $v(r)$ through

$$a = \pi \int_{2r_0}^{\infty} |v(r)|^2 r^2 dr \quad , \quad b = \frac{16}{3} \pi r_0^3 \quad , \quad (3)$$

where $2r_0$ denotes the radius of the repulsive core (see fig.1).

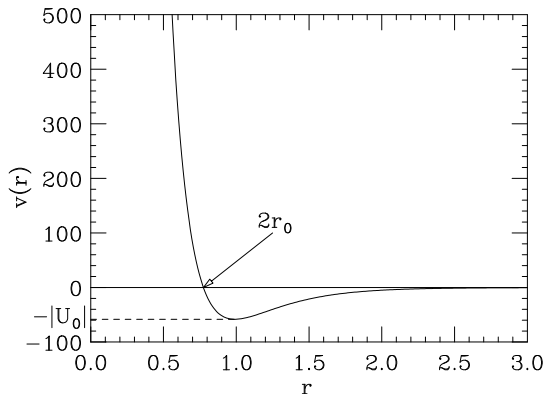


Figure 1. Behavior of the potential describing the interactions between constituents of a van der Waals fluid (the interparticle distance r and $v(r)$ are both given in arbitrary units).

In spite of its simplicity, the van der Waals EOS describes most of the features of both the gas and liquid phases of the system, as well as the nature of the phase transition.

The EOS of strongly interacting matter reflects the complexity of the underlying dynamics, that makes the phase diagram extremely rich. As an example, fig.2 shows the phase diagram of charge neutral strongly interacting matter in β -equilibrium².

In this talk, I will review the available empirical information on the EOS of strongly interacting matter at $T \sim 0$, and the extent to which this information can be used to constrain theoretical models. The knowledge coming from nuclear systematics and neutron stars data is summarized in Sections 2 and 3, respectively. Section 4 provides a short overview of the theoretical models of neutron star matter at supranuclear density, while Section 5 is devoted to the prospects for obtaining new insights from the experimental study of gravitational waves emitted by neutron stars. Finally, Section 6 summarizes the main results and states the conclusions.

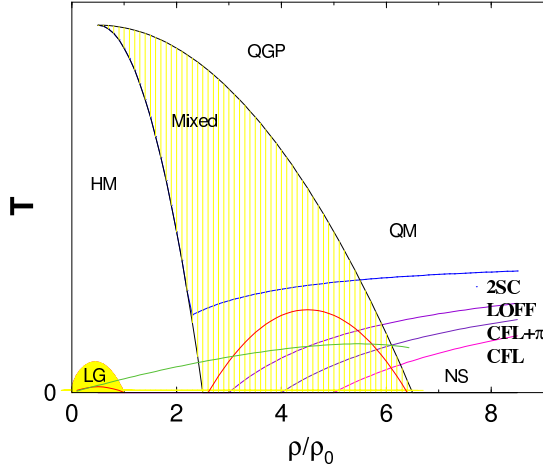


Figure 2. Temperature *vs* baryon density phase diagram of charge neutral strongly interacting matter in β -equilibrium. Hatched areas correspond to mixed phases of hadronic matter (HM) and quark matter (QM/QGP), as well as the nuclear liquid-gas (from ref.²).

2 Constraints on the EOS at $T=0$ from nuclear data

Under standard terrestrial conditions, strongly interacting matter is observed in form of rather small, cold chunks: the atomic nuclei.

Nuclei are self-bound systems consisting of Z protons and $(A - Z)$ neutrons. Their smallness is a consequence of the electrostatic repulsion between protons, limiting A to ~ 200 , while the fact that they can be described as cold objects follows from the observation that thermal energies are negligible in comparison to the large proton and neutron Fermi energies.

The body of data on nuclear masses provides a constraint on the density dependence of the energy per particle $e = E/A$ at zero temperature, related to the EOS through

$$P(n, T = 0) = - \left(\frac{\partial E}{\partial \Omega} \right)_{T=0} = n^2 \left(\frac{de}{dn} \right)_{T=0}. \quad (4)$$

The A -dependence of the nuclear binding energy (i.e. the difference between the measured nuclear mass and the sum of the constituent masses) is well described by the semiempirical formula

$$B(Z, A) = a_V A + a_s A^{2/3} + a_c \frac{Z^2}{A^{1/3}} + a_A \frac{(A - 2Z)^2}{4A} - \lambda a_p \frac{1}{A^{1/2}}, \quad (5)$$

whose terms account for nuclear interactions, taking place both in the interior of the nucleus and on its surface, electrostatic interactions between protons, isospin asymmetry and shell effects.

The coefficient of the term linear in A yields the binding energy of *symmetric nuclear matter*, an ideal uniform system consisting of equal number of protons and neutrons coupled by strong interactions only. The equilibrium density of such a system, n_0 , can be inferred exploiting saturation of nuclear densities, i.e. the fact that the central density of atomic nuclei, measured by elastic electron-nucleus scattering, does not depend upon A for large A .

The empirical equilibrium properties of nuclear matter are

$$e_0 = e(n = n_0, T = 0) = -16 \text{ MeV}/A \quad , \quad n_0 \sim .16 \text{ fm}^{-3} . \quad (6)$$

In the vicinity of the equilibrium density $e(n, T = 0)$ can be expanded according to (as we will only discuss the EOS at $T = 0$, the dependence upon T will be omitted hereafter)

$$e(n) \approx e_0 + \frac{1}{2} \frac{K}{9} \frac{(n - n_0)^2}{n_0^2} , \quad (7)$$

where

$$K = 9 n_0^2 \left(\frac{\partial^2 e}{\partial n^2} \right)_{n=n_0} = 9 \left(\frac{\partial P}{\partial n} \right)_{n=n_0} \quad (8)$$

is the (in)compressibility module, that can be extracted from the measured excitation energies of nuclear vibrational states. Empirical values range from $K \sim 200$ MeV (corresponding to more compressible nuclear matter, i.e. to a *soft* EOS) to $K \sim 300$ MeV (corresponding to a *stiff* EOS) ³.

It has to be emphasized that the quadratic extrapolation of Eq.(7) cannot be expected to work far from equilibrium density. In fact, assuming a parabolic behavior of $e(n)$ at large n ($\gg n_0$) leads to predict a speed of sound in matter, v_s , larger than the speed of light, i.e.

$$\left(\frac{v_s}{c} \right) = \frac{1}{n} \left(\frac{\partial P}{\partial e} \right) > 1 , \quad (9)$$

regardless of the value of K .

Eq.(9) shows that causality requires

$$\left(\frac{\partial P}{\partial \epsilon} \right) < 1 , \quad (10)$$

where $\epsilon = E/\Omega$ is the energy-density. For a noninteracting Fermi gas $\epsilon \propto n^{4/3}$, implying (the equal sign corresponds to massless fermions)

$$P \leq \frac{\epsilon}{3}, \quad \left(\frac{v_s}{c}\right) \leq \frac{1}{3}. \quad (11)$$

In presence of interactions the above limits can be easily exceeded. For example, modeling the repulsion between nucleons in terms of a rigid core leads to predict infinite pressure at finite density.

The stiffest EOS compatible with causality is $P = \epsilon$, corresponding to $(v_s/c) = 1$. Back in the early 60's Zel'dovich was able to show that the $v_s = c$ limit, corresponding to $\epsilon \propto n^2$, is indeed attained in a simple semirealistic theory, in which nucleons are assumed to interact through exchange of a vector meson ⁴.

3 Constraints on the EOS at $T=0$ from neutron stars data

At very large A ($\sim 10^{57}$), gravity becomes strong enough to balance the repulsive interactions between nucleons, and nuclear matter can occupy macroscopic regions of space. This is the situation occurring in the interior of neutron stars, compact astrophysical objects (typical values of mass and radius are $\sim 1.4 M_\odot$ and ~ 10 Km, respectively) whose central density largely exceeds n_0 . The structure of a neutron star is schematically represented in

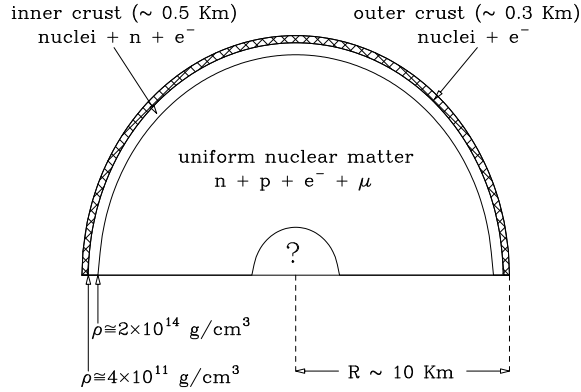


Figure 3. Cross section of a neutron star. Note that the equilibrium density of nuclear matter corresponds to $\sim 2.7 \times 10^{14}$ g/cm³.

fig.3. Note that the inner and outer crusts contain a comparatively small

amount of matter, most of the star mass being concentrated in the region of supranuclear densities ($n > n_0$). In addition, as all relevant Fermi energies are much larger than the typical temperature ($\lesssim 10^9$ K ~ 100 KeV), neutron stars can be regarded as cold object. The main features of the theoretical models of neutron star matter will be summarized in Section 4.

Given the EOS describing matter in the interior of a neutron star, its mass and radius can be obtained from the Tolman-Oppenheimer-Volkov (TOV) equations

$$\frac{dP(r)}{dr} = -G \frac{[\epsilon(r) + P(r)/c^2] [M(r) + 4\pi r^2 P(r)/c^2]}{r^2 [1 - 2GM(r)/rc^2]} . \quad (12)$$

$$M(r) = 4\pi \int_0^r r'^2 dr' \epsilon(r') , \quad (13)$$

In the above equations, combining hydrostatic equilibrium with Einstein's equations of general relativity for a nonrotating star, P and ϵ denote pressure and energy-density, respectively, and G is the gravitational constant.

For any value of the central energy-density $\epsilon_c = \epsilon(r = 0)$ Eq.(12) can be integrated outward until the star radius R , defined by the condition $P(R) = 0$, is reached. The star mass $M(R)$ can then be obtained from Eq.(13).

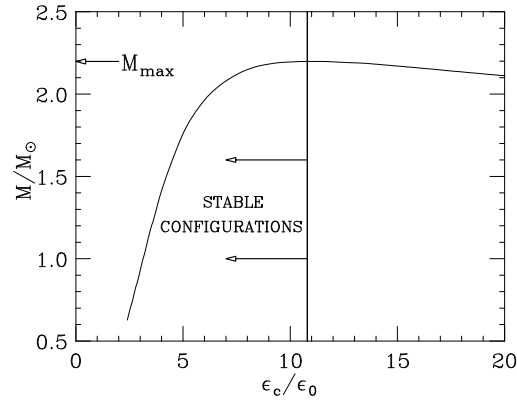


Figure 4. Typical dependence of the neutron star mass (in units of the solar mass M_\odot) upon the energy-density at the center of the star (in units of the energy-density of symmetric nuclear matter at equilibrium).

Fig.4 shows the typical behavior of the neutron star mass as a function

of the central energy-density. Denoting by $\bar{\epsilon}$ the central energy-density corresponding to the maximum mass, all stable configurations have $\epsilon_c < \bar{\epsilon}_c$.

The value of the maximum mass is mostly determined by the *stiffness* of the EOS, more incompressible neutron star matter (i.e. *stiffer* EOS) corresponding to larger M_{max} . Therefore, in principle measurements of neutron star masses may provide information on the behavior of the EOS at $n > n_0$.

The most precise experimental data, obtained from studies of the timing of radio pulsars, yield the average value ⁵

$$M = 1.35 \pm 0.04 M_{\odot} , \quad (14)$$

thus constraining any realistic model of EOS to support a stable star with mass $\sim 1.4 M_{\odot}$.

Neutron star masses can also be obtained from the analysis of binary systems containing an X-ray pulsar. A recent determination of the mass of the Vela X-1 pulsar yields $M = 1.86 \pm 0.33 M_{\odot}$ ⁶, suggesting the possibility of a mass well above the canonical value of Eq.(14). If confirmed, the existence of a neutron star with $M > 1.8M_{\odot}$ would provide a very stringent constraint, ruling out theoretical models that predict very soft EOS.

4 Theoretical models of neutron star matter at supranuclear density.

Theoretical models of neutron star matter are based on different approaches, involving different degrees of freedom, which are expected to be applicable in different density regimes.

In the range $n_0 \lesssim n \lesssim 4n_0$ matter in the interior of the star is believed to take the form of a cold uniform fluid, that can be described in terms of hadronic degrees of freedom, within the framework of either nonrelativistic many-body theory⁷ or relativistic mean-field approaches⁸.

At n just above n_0 neutrons dominate, with a small fraction of protons and leptons in equilibrium with respect to the weak interaction processes (ℓ denotes either an electron or a muon)

$$n \rightarrow p + \ell + \bar{\nu}_{\ell} \quad , \quad p + \ell \rightarrow n + \nu_{\ell} . \quad (15)$$

For any baryon density n , minimization of the total energy-density with the constraints of baryon number conservation and charge neutrality fixes the relative abundances of neutrons, protons and leptons. Note that, as the proton fraction is small, typically $< 10\%$, theoretical calculations of the EOS involve the study of strongly *asymmetric* nuclear matter, whose energy is most sensitive to the isospin asymmetry term in Eq.(5). The importance of isospin

asymmetry is illustrated in fig.5, showing the calculated density dependence of the energy per particle of symmetric nuclear matter ($(Z/A) = 1/2$) and pure neutron matter ($(Z/A) = 0$). It clearly appears that unlike symmetric nuclear matter, whose energy exhibits a minimum, pure neutron matter is not self-bound at any density.

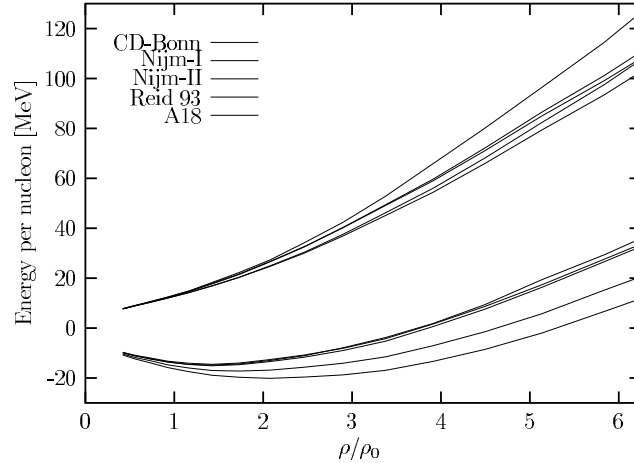


Figure 5. Typical density dependence of the energy per nucleon of pure neutron matter (upper curves) and symmetric nuclear matter (lower curves), obtained from nonrelativistic nuclear many-body approaches⁷. The density is given in units of the equilibrium density of symmetric nuclear matter.

As the density increases, different forms of matter, containing hadrons other than protons and neutrons, can become energetically favored. For example, the weak interaction process



leading to the appearance of a strange baryon, sets in as soon as the sum of the electron and neutron chemical potentials exceeds M_{Σ^-} (typically at $n \gtrsim 2n_0$). At larger density the production of Λ^0 's is also energetically allowed.

For any fixed baryon density, the relative abundances of the different hadronic and leptonic species are dictated by the requirements of equilibrium with respect to weak interactions, conservation of baryon number and charge neutrality. Fig.6 shows the particle fractions resulting from the nonrelativistic many-body approach of ref.⁹.

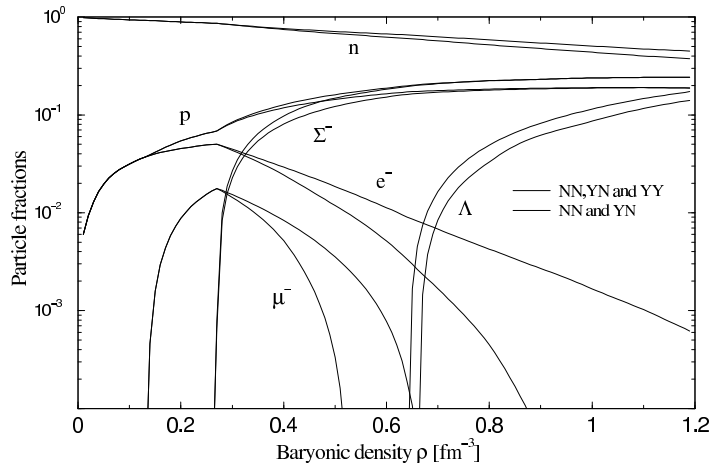


Figure 6. Relative abundances of hadrons and leptons in a hadronic model of neutron star matter (taken from ref.⁹).

The transition from nucleon matter to hadronic matter is associated with a softening of the EOS, as it basically amounts to replacing particles carrying large Fermi energies with more dilute, and therefore less energetic, strange baryons. Hence, using the EOS of hadronic matter as an input for the solution of the TOV equations leads to predict a value of the maximum mass significantly lower than that obtained using nucleon matter.

At very large density ($n > 4n_0$) a new transition, to a phase in which quarks are no longer clustered into nucleons or hadrons, is eventually expected to take place. In most theoretical studies of neutron stars structure, the EOS of quark matter has been estimated using the simple MIT *bag model* (for a recent review see ref.¹⁰).

The bag model assumes that quarks be confined to a finite region of space (the bag), whose volume is limited by a pressure B (the bag constant). Its simplest implementation includes only massless and noninteracting u and d quarks. Equilibrium with respect to the process (ℓ denotes either an electron or a muon)

$$d \rightarrow u + \ell + \bar{\nu}_\ell, \quad (17)$$

requires that the u and d chemical potentials satisfy (note that, as the mean free path of neutrinos in dense nucleon matter largely exceeds their typical

radius, neutron stars can be regarded as transparent to neutrinos)

$$\mu_d = \mu_u + \mu_\ell \quad , \quad \mu_e = \mu_\mu, \quad (18)$$

whereas the constraint of charge neutrality implies

$$\frac{2}{3}n_u = \frac{1}{3}n_d + n_e + n_\mu, \quad (19)$$

where n_q ($q = u, d$) and n_ℓ ($\ell = e, \mu$) denote the quark and lepton densities, respectively.

The energy-density reads

$$\epsilon = \frac{E}{\Omega} = B + \frac{3}{4\pi^2} \sum_q p_{F_q}^4, \quad (20)$$

and the quark Fermi momenta are related to the total baryon density n through

$$p_{F_q} = (\pi^2 f_q n)^{(1/3)}, \quad (21)$$

f_q being the number of quarks of flavor q per baryon. Finally, the pressure can be readily obtained from

$$P = - \left(\frac{\partial E}{\partial \Omega} \right) = -B + \frac{1}{4\pi^2} \sum_q p_{F_q}^4. \quad (22)$$

More realistic models include a massive strange quark and allow for one-gluon exchange interactions between quarks of the same flavor. At fixed baryon density the quark and lepton fractional densities are determined by the requirements of chemical equilibrium, charge neutrality and baryon number conservation. Fig.7 shows the results obtained including massless u and d quarks and strange quarks of mass $m_s = 150$ MeV, neglecting all interactions and setting the value of the bag constant to $B = 208$ MeV/fm³.

In the $n \rightarrow \infty$ limit, the energy per baryon of nucleon matter, e_{NM} , grows linearly with baryon density, whereas in quark matter $e_{QM} \sim n^{1/3}$. Hence, a transition from nucleon to quark matter is expected to take place in the inner region of neutron stars, provided the central density is large enough.

In the simplest implementation, the phase transition is assumed to take place at constant pressure and chemical potential, so that matter density exhibits a discontinuity at the boundary between the two phases. According to this picture the star consists of a core of quark matter surrounded by nucleon matter.

The calculations of ref.¹¹, based on nonrelativistic many-body theory for the description of nucleon matter and the bag model for the description of

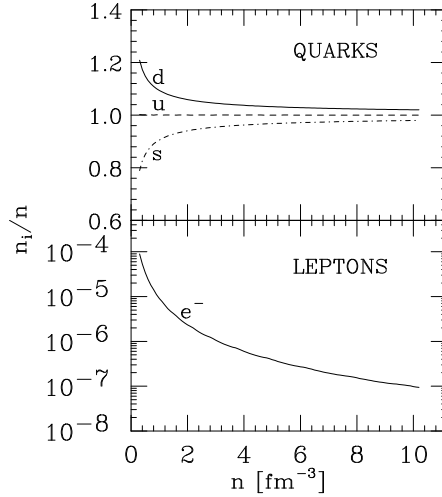


Figure 7. Relative abundances of quarks and leptons in β -stable matter consisting of massless u and d quarks and strange quarks with mass $m_s = 150$ MeV. All interactions between quarks are neglected and the bag constant is set to $B = 208$ MeV/fm³.

quark matter, predict a transition region $5.4 < (n/n_0) < 9.8$ for $B = 200$ MeV/fm³ and $4.9 < (n/n_0) < 7.5$ for $B = 122$ MeV/fm³.

The transition to quark matter makes the EOS softer, thus lowering the value of the maximum neutron star mass. The authors of ref.¹¹ report a reduction ΔM_{max} of $\sim 10\%$ and $\sim 20\%$ for $B = 200$ and 122 MeV/fm³, respectively.

5 Will detection of gravitational provide new insight ?

As the pattern of nonradial oscillations of neutron stars depends upon the EOS describing matter in the interior of the star, detection of gravitational wave emission associated with the excitation of these modes can in principle provide additional constraints on theoretical models of the EOS.

For example, the complex oscillation frequencies of the axial (i.e. odd parity) modes of a nonrotating star are eigenvalues of a Schrödinger-like equation whose potential $V_\ell(r)$ explicitly depend upon the EOS according to¹²

$$V_\ell(r) = \frac{e^{2\nu(r)}}{r^3} \{ \ell(\ell+1)r + r^3 [\epsilon(r) - P(r)] - 6M(r) \} , \quad (23)$$

where

$$\frac{d\nu}{dr} = -\frac{1}{[\epsilon(r) + P(r)]} \frac{dP}{dr} . \quad (24)$$

Using realistic EOS one obtains strongly damped eigenmodes, called *w-modes*, whose frequencies exhibit the behavior displayed in fig.8.

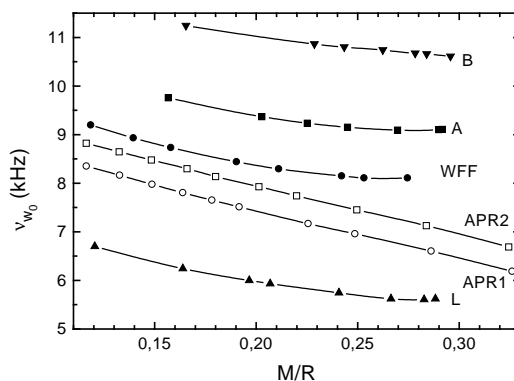


Figure 8. Frequencies of the first axial *w*-mode of a nonrotating neutron star, plotted as a function of the star compactness (M/R). The different curves correspond to different models of EOS (taken from ref.¹²).

The pattern of frequencies strictly reflects the stiffness of the different EOS in the relevant density region (typically $1 < (n/n_0) < 5$, softer EOS corresponding to higher frequencies. For example, the curve labelled B has been obtained from a model including nucleons, nucleon excitations and strange baryons, predicting a very soft EOS and a maximum mass of $1.42 M_{\odot}$.

It is interesting to note that the dependence upon the the ratio (M/R) is rather weak, so that detection of a given frequency may allow one to discriminate between different models of EOS (e.g. between model B, corresponding to hadronic matter and model WFF, corresponding to nucleon matter) regardless of the compactness of the star.

A different class of nonradial oscillations, the *g-modes*, are associated with the occurrence of a density discontinuity in the interior of the star. Early studies of these modes focused on discontinuities that are known to be produced by the changes of chemical composition in the low density region of the crust, corresponding to a fractional distance from the surface (d/R) $\lesssim 10\%$.

As pointed out in Section 4, a different discontinuity may be produced by the transition from nucleon to quark matter, which is expected to take place at much larger density and involve a much larger density jump.

It has to be emphasized that, as nucleon and quark matter need not to be considered independently charge neutral, in general the deconfinement transition may involve the occurrence of a mixed phase (e.g. bubbles of quark matter in nucleon matter at lower density or *viceversa* at larger density) extending over a sizable region of space, rather than a sharp separation between the two phases¹⁰. Whether the mixed phase is energetically favored depends upon the balance between the gain in volume energy and the loss associated with Coulomb and surface energy¹³. If Coulomb and surface energies prevail, a density discontinuity is expected to occur.

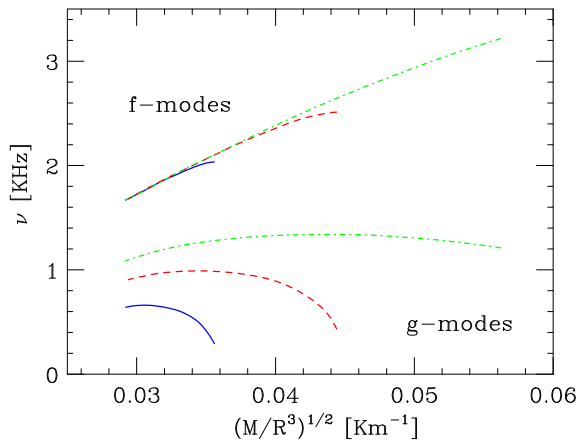


Figure 9. Frequencies of the f- and g-mode of a neutron star of mass $M = 1.4M_{\odot}$ as a function of the average density. Solid, dashed and dot-dash lines correspond to density jumps of 10 %, 20 % and 30 %, respectively. All stellar models have polytropic exponent $\Gamma = 2$ (see Eq.(25))¹⁴

The authors of ref.¹⁴ have recently carried out an exploratory calculation of the frequencies of both the fundamental f-mode and the g-mode of a nonrotating neutron star, using a simple polytropic EOS with a density discontinuity Δn located at density $n = n_D$:

$$P(n) = \begin{cases} K \left(1 + \frac{\Delta n}{n_D}\right)^{\Gamma} n^{\Gamma} & n < n_D \\ Kn^{\Gamma} & n > n_D + \Delta n . \end{cases} \quad (25)$$

The results of ref.¹⁴ are summarized in fig.9, showing the f- and g-mode frequencies as a function of the average density of the star, whose mass is kept fixed at the canonical value of $1.4 M_{\odot}$. It clearly appears that, while the f-mode frequency exhibits a nearly linear growth, largely unaffected by the abrupt structural change associated with the phase transition, the frequencies of the g-mode strongly depend upon the jump in density Δn . Hence, a simultaneous measurements of the frequencies of the two modes would provide information on both size and location of the discontinuity.

6 Conclusions

The extent to which the currently available empirical information constrains the EOS of cold β -stable strongly interacting matter is illustrated in fig.10.

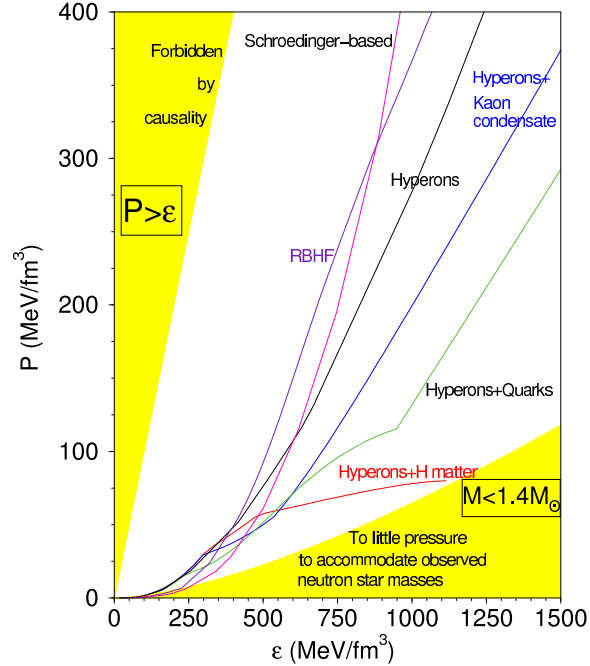


Figure 10. EOS of cold β -stable strongly interacting matter resulting from a variety of different theoretical approaches, based on both hadronic and quark degrees of freedom. The shaded areas show the region forbidden by causality and that corresponding to $M_{max} < 1.4 M_{\odot}$ (taken from ref.¹⁵).

Although all EOS resulting from nonrelativistic approaches are known to be plagued by a noncausal behaviour at very large density, it appears that the constraint $P > \epsilon$ is fulfilled by all EOS over a wide range of energy-density.

The requirement that the maximum mass be larger than $1.4 M_{\odot}$ does not provide a stringent constraint either, as all reasonable models support a stable star with $M = 1.4 M_{\odot}$. However, as pointed out in Section 3, the situation may change should the mass of the Vela X-1 pulsar be confirmed to be larger than $1.8 M_{\odot}$. In this case the shaded region in the lower right corner of fig.10 would considerably extend upward, thus ruling out models that predict very soft EOS.

The observation of gravitational waves emitted by neutron stars may provide valuable new insight, allowing to further constrain theoretical models. Detection of gravitational radiation in the relevant few KHz frequency range may become possible with the recently proposed gravitational laser interferometric detector EURO¹⁶.

As far as theory is concerned, it has to be mentioned that the recent progress in Quantum Monte Carlo has made it possible to apply this approach to the study of the EOS of pure neutron matter¹⁷. The extension to the case of β -stable matter, that appears to be feasible, would be of great importance for the understanding of neutron star matter in the region of not too high density ($n \lesssim 2n_0$), where the use of nucleonic degrees of freedom is likely to be reasonable.

At larger densities a transition to quark matter is expected to take place. A better theoretical description of this region will require a careful analysis of the nature of the phase transition as well as a more realistic description of the deconfined phase. In this context, a pivotal role is likely to be played by detailed quantitative studies of the possible occurrence of the color superconducting phase predicted by the fundamental theory of strong interactions¹⁸.

References

1. K. Huang *Statistical Mechanics* (Wiley, New York, 1963).
2. H. Heiselberg, talk given at the Workshop on "Compact Stars in the QCD Phase Diagram", Copenhagen, August 15-18, 2001. astro-ph/0201465.
3. S. Shlomo and D.H. Youngblood, *Phys. Rev. C* **47**, 529 (1993).
4. Ya. B. Zel'dovich, *Sov. Phys. JETP* **14**, 1143 (1962).
5. S.E. Thorsett and D. Chakrabarty, *ApJ* **512**, 288 (1999).
6. M.H. van Kerkwijk, astro-ph/0110336.
7. H. Heiselberg and V.R. Pandharipande, *Ann. Rev. Nucl. Part. Sci.*, **50**, 481 (2000).

8. N.K. Glendenning, *Compact Stars* (Springer, New York, 1997).
9. I. Vidaña *et al*, *Phys. Rev. C* **62**, 035801 (2000).
10. H. Heiselberg and M. Hjorth-Jensen, *Phys. Rep.* **328**, 237 (2000).
11. A. Akmal, V.R. Pandharipande and D.G. Ravenhall, *Phys. Rev. C* **58**, 1804 (1998).
12. O. Benhar, E. Berti and V. Ferrari, *Mon. Not. R. Astron. Soc.* **310**, 797 (1999).
13. H. Heiselberg, C.J. Pethik and E.F. Staubo, *Phys. Rev. Lett.* **70**, 1355 (1993).
14. G. Miniutti, J.A. Pons, E. Berti, L. Gualtieri and V. Ferrari, paper in preparation.
15. F. Weber, *Pulsars as Astrophysical Laboratories for Nuclear and Particle Physics* (IoP Publishing, Bristol, 1999).
16. EURO: Europe's Third Generation Gravitational Wave Observatory. Proposal available at <http://carina.astro.cf.ac.uk/geo/euro/> (May, 2000).
17. K.E. Schmidt and S. Fantoni, *Phys. Lett.* **B446**, 99 (1999).
18. M.G. Alford, K. Rajagopal, S. Reddy and F. Wilczek, *Phys. Rev. D* **64**, 074017 (2000).